J Nanostruct 16(1): 808-816, Winter 2026

RESEARCH PAPER

Study the Structural and Morphological Properties of (Cu /Ag) doped TiO_2 Nanoparticle Prepared via Solvothermal Method

Basma Abbas Jabbar [1,2]*, Noor J. Ridha [1], Khawla J. Tahir [1]

[1] Department of Physics, College of Science, University of Kerbala, Iraq

[2] Department of Medical Physics, College of Applied Medical Sciences, University of Kerbala, Iraq

ARTICLE INFO

Article History:
Received 16 September 2025
Accepted 23 December 2025
Published 01 January 2026

Keywords:
Cu/Ag doped titanium
Optical properties
Solvothermal method
Structural properties

ABSTRACT

Doping metals with titanium dioxide (TiO_2) has gained significant attention due to its ability to enhance the properties and performance of various metal- based materials in several fields such as catalysis, energy storage and environmental applications. In this study, pure TiO_2 as well various concentrations of copper (Cu) and silver (Ag) doped TiO_2 nanoparticles were synthesized by solvothermal method using Titanium (IV) tetra-isopropoxide as precursors. The TiO_2 samples were prepared as follow: pure TiO_2, TiO_2 doped with 1.5% Cu:1% Ag, 1% Cu:1.5% Ag and 1% Cu:1% Ag nanoparticles named as, T_0, T_1, T_2 and T_3, respectively. The samples were annealed at 500 °C for 2 hours and characterized by X-ray diffraction (XRD), Fourier transform infrared (FTIR), field emission scanning electron microscopy (FESEM), energy dispersive Xray-spectroscopy (EDX) and photoluminescence spectroscopy (PL). The results of XRD indicated that doping TiO_2 with Cu and Ag ions leads to a reduction in average crystallite size compered to pure TiO_2, the average crystallite size of T_0, T_1, T_2 and T_3 were found to be 13.56, 12.73, 13.03 and 12.67 nm, respectively. FESEM imaging revealed spherical nanoparticles with little agglomeration, while EDX analysis confirmed the successful incorporation of Cu and Ag into the TiO_2 matrix, with distinct peaks corresponding to Ti, O, Cu and Ag. The results of PL show that the Cu/Ag-doped TiO_2 nanoparticles decrease the recombination rate of photo-induced electron–hole pairs.

How to cite this article
Abbas Jabbar B., J Ridha N., J. Tahir K. Study the Structural and Morphological Properties of (Cu /Ag) doped TiO_2 Nanoparticle Prepared via Solvothermal Method. J Nanostruct, 2026; 16(1):808-816. DOI: 10.22052/JNS.2026.01.071

INTRODUCTION

Nanotechnology has opened new ways to modify material properties in recent decades to satisfy certain scientific and technological demands [1]. Because of their remarkable photocatalytic characteristics, (TiO_2) nanoparticles have emerged as a center of attention of scientific investigation among these materials [2]. TiO_2 has attracted an enormous amount of interest lately because of its non-toxic properties, high chemical stability [3], high optical transmission and enhanced photo-catalytic performance [4], good durability, high dielectric constant and high refractive index [5,6]. TiO_2 has also been regarded as a promising material due to its electrical properties [7] [8] and it can be utilized in extensive range of applications, such as solar cells [9], gas sensors [10] and photo-catalysis systems [11]. Due to its wide band gap (3.2 eV), TiO_2 has limited optoelectronic applications in the visible region of the spectrum [12].

* *Corresponding Author Email: basma.a@uokerbala.edu.iq*

Recently, metal doping has been applied to improve the physical and chemical properties of TiO_2 nano-fibers and nanoparticles (NPs) [13]. The electronic structural and optical properties of TiO_2 particles are modified by doping metal and nonmetal ions to enhance the efficiency of interfacial charge transfer, slow down the recombination rate of the electron-hole pairs, and enhance their response [14]. Additionally, metal doping might affect the crystal structure of titania, which would improve the application fields significantly [13].

Doping TiO_2 with metals such as silver (Ag) and copper (Cu) is applied to improve its photo-catalytic performance, particularly under visible light, and to enhance its antimicrobial properties [15, 16]. Ag ion is used to improve the photo-catalytic activity of TiO_2 through surface plasmon resonance (SPR), which assists in the absorption of visible light, thus extending TiO_2 photo-catalytic performance beyond its usual ultraviolet (UV) absorption range. This leads to a more effective generation of electron-hole pairs for photo-catalytic [17, 18]. On the other hand, Cu modulates the electronic structure of TiO_2, allowing to enhance light absorption in the visible spectrum and to reduce electron-hole recombination [19]. Furthermore, Cu doping produces oxygen vacancies that improve photo-catalytic efficiency [20]. Moreover, both Ag and Cu doping contribute to TiO_2 antimicrobial properties, making it useful for environmental and biomedical applications such as water purification and self-cleaning surfaces [21] [22]. Various methods such as chemical deposition [23], sol–gel [24], hydrothermal [25], microwave [26], and solvothermal synthesis [27] have been used to synthesis pure and doped TiO_2 NPs with metals.

In this work, (copper and silver)-doped titania (Cu/Ag-TiO_2) NPs have been synthesized by solvothermal method at annealing temperature 500 °C. On the other hand, the influence of doping on the structural and morphological characteristics of the modified titania has been investigated.

MATERIALS AND METHODS

Chemicals

Titanium (IV) tetra-isopropoxide (TTIP, 97 % Aldrich Company), Copper (II) nitrate trihydrate ($Cu(NO_3)_2.3H_2O$), 99 %, Silver Nitrate ($AgNO_3$), Ethanol (C_2H_5OH, 99.5 %) and deionized water (DI) were used in synthesis of (Cu/Ag) doped TiO_2 NPs.

Synthesis of (Cu/Ag) doped TiO_2 nanoparticles

To prepare TiO_2 NPs, two distinct solutions were prepared: solution A and solution B. Solution A was formed by mixing 5 ml of (TTIP) with 25 ml of ethanol. To ensure homogeneity, the solution was vigorously stirred for 15 min at room temperature. Meanwhile, solution B was prepared by mixing 25ml of ethanol and 5ml of distilled water. To synthesis (Cu/Ag) doped TiO_2 NPs, this step was followed by the preparation of solution C. Hence

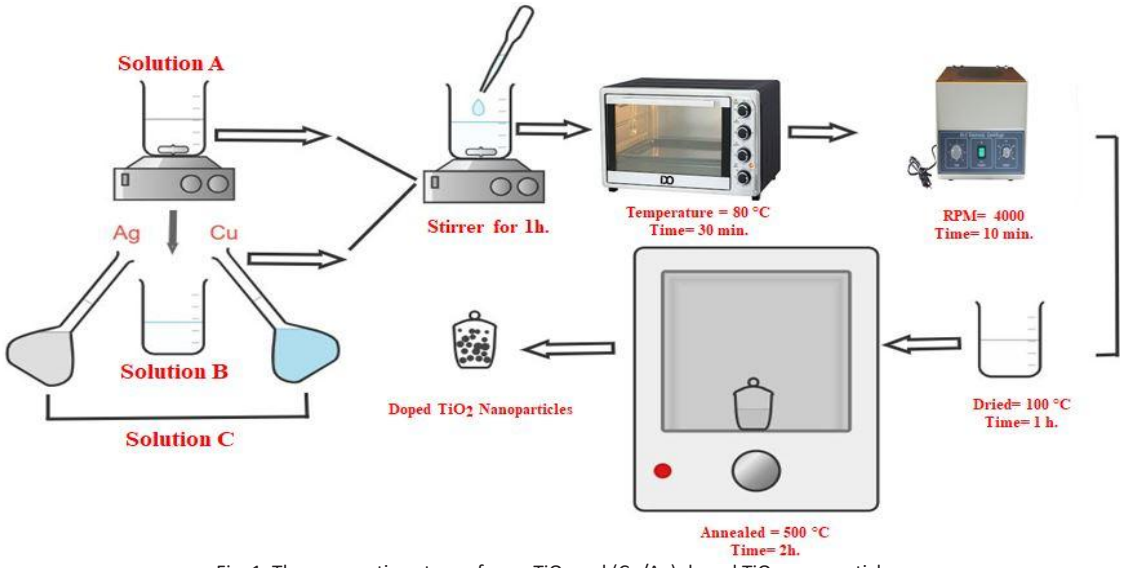

Fig. 1. The preparation steps of pure TiO_2 and (Cu/Ag) doped TiO_2 nanoparticles.

the aqueous solutions of specific amounts from (1.5, 1, 1%) wt. of $Cu(NO_3)_2.3H_2O$ and (1, 1.5, 1%) wt. of ($AgNO_3$) were both added drop-wise to solution B. Next, solution C was added drop-wise to solution A with continuous vigorous stirring for 1 hour. The final solution was then placed in an oven at 80 °C for 30 min. Then, the precipitate was centrifuged and washed 4 to 5 times with distilled water and ethanol in order to remove the impurities from the solution at 4000 rpm for 10 min. The resulting precipitate was dried under vacuum conditions in an oven at 100 °C for 1 hour. Finally, the generated white powder samples were annealed at 500 °C for 2 hour. In this work, the prepared samples of pure and doped TiO_2 NPs with (1.5% Cu:1% Ag), (1% Cu:1.5% Ag) and (1% Cu:1% Ag) will be indicated as T_0, T_1, T_2 and T_3, respectively. Fig. 1 illustrates the preparation steps of the un-doped and (Cu/Ag) doped TiO_2 NPs via solvothermal method.

Characterizations

Powder (XRD) patterns of the synthesized samples were recorded in the range 2θ° of 10–80°, operating at 40 kV of voltage and 40 mA of current. The XRD source was a Cu anode with a Cu-Kα1 (λ =1.54060 Å) radiation. The Crystallite size and (D) was calculated using the Scherer equation [28]:

$$D = \frac{K\lambda}{\beta \cos\theta} \quad (1)$$

where K denotes the shape factor (= 0.9), λ is the incident X-ray wavelength, β represents the full width at half maximum (FWHM) and θ is the diffraction angle at the peak maximum of the determined plane.

To determine the lattice parameters (a, b, and c) of the samples, the following formulas (pertaining to the tetragonal crystal system) were used [29]:

$$\frac{1}{d^2} = \frac{h^2+k^2}{a^2} + \frac{l^2}{c^2} \quad (2)$$

In this equation, d represents the inter-planar spacing, and (h, k, l) refer to the Miller indices. The lattice constants, *a* and *c*, were determined from the lattice spacing of the anatase peaks observed at the (101) and (200) planes. This calculation was based on the Bragg equation for a tetragonal lattice structure, where the *a* and *b* values are equal, but the *c* value differs. From the lattice constants (*a* and c), the unit cell volume (V) of the samples can be calculated from the following relation [29]:

$$V = a^2.c \quad (3)$$

Morphological characterization was conducted using filed emission scanning electron microscopy (FESEM, MIRA3TESCAN, 15keV). The samples were placed on a conductive carbon tape and subsequently coated with a thin layer of gold in a vacuum environment. The size distributions of the examined nanostructures, was obtained from filed emission scanning electron microscopy (FESEM) images, using Image J software. A fluorescence spectrometer (Hitachi F4500, Tokyo, Japan) was utilized to measure the luminescence characteristics of the synthesized composite materials. FTIR analysis of TiO_2 and Cu-Ag-TiO_2 NPs was conducted using the Attenuated Total Reflectance (ATR) mode with the IR Tracer100 Shimadzu as an accessory. Prior to the analysis, a background scan was performed. The spectra were recorded within the range of 4000 to 400 cm^{-1}, utilizing a resolution of 8 cm^{-1}, and averaged over 256 scans.

RESULTS AND DISCUSSION

X-Ray Diffraction (XRD) analysis

The structural characteristics and nanoparticle's phase of the synthesized samples were studied using XRD. The XRD patterns of pure and doped TiO_2 (T_0, T_1, T_2 and T_3) NPs were shown in Fig. 2. The existence of the anatase phase was confirmed by the peaks at 25.47°, 37.04°, 37.91°, 38.63°, 48.17°, 54.08°, 55.19°, 62.80°, 68.78°, 70.36° and 75.10° corresponding to planes (101), (103), (004), (112), (200), (105), (211), (204), (116), (220), and (215), respectively, according to the reference JCPDS data (01-073-1764).

Although there were missing peaks related to Ag and Cu, nevertheless the main diffraction peaks shifted toward the lower 2θ value and broaden with increasing doping ion concentration which may be due to lattice strain present in the samples. The ionic radius of Cu^{2+} (0.72 Å) is slightly greater than that of Ti^{4+} (0.68 Å). Thus, it is possible to substitute small amounts of Ti^{4+} instead of Cu^{2+} in the structure, which could be accompanied by a weak lattice expansion, generated by the small difference between its ionic radii [30] [31]. However, it is improbable that Ag^+ could replace Ti^{4+} in the TiO_2 matrix because the Ag^+ ion radius (1.26 Å) is larger than that of Ti^{4+} (0.68 Å), which would generate a significant lattice expansion. Therefore, it is less probable to find Ag^+ within

the TiO_2 crystal lattice. Consequently, silver is presumed to be present as Ag NPs on the materials surface [32]. The absence of distinct Ag and Cu peaks in the XRD analysis after doping with TiO_2 suggests that silver and copper are either present in an amorphous state, highly dispersed within the TiO_2 matrix, or incorporated into the TiO_2 lattice as substitutional or interstitial species.

The results showed that the average crystallite size reduced as a result of the TiO_2 NPs doping, as shown in Table 1. The introduction of dopant ions into the TiO_2 lattice was responsible for this decrease in crystallite size because it caused lattice strain, which inhibited crystal growth, leading to smaller crystallites.

Fourier transform infrared (FTIR) analysis

FTIR is the most suitable method for examining changes in structures, bond vibrations, and interactions within the material. Fig. 3 shows the FT-IR spectra of the different wt. % of Cu-Ag doped Titania NPs compared to pure TiO_2 over the wavenumber range of 400 cm^{-1} to 4000 cm^{-1}. It is demonstrated that the synthesized nanoparticles exhibit multiple absorption bands, which show distinct variations in their intensities. The FT-IR spectra indicated that the absorption characteristics of all synthesized nanoparticles exhibit a similar pattern, with no distinct new absorption bands. The large peak in the region from 2200 cm^{-1} to 2400 cm^{-1} explains the C– O bands [33]. The strong peak at the region from 1000 cm^{-1} to 1500 cm^{-1} was corresponds to O–H bond stretching vibrations group [34]. The peak in the range 500 cm^{-1} to 900 cm^{-1} was attributed to the stretching vibration of the Ti-O bond [32].

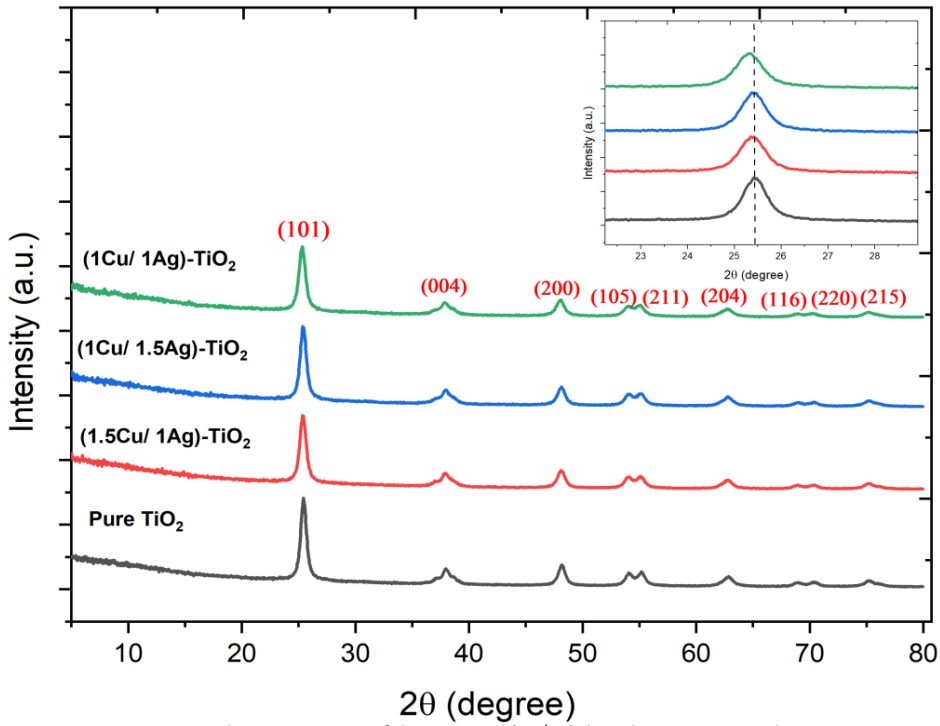

Fig. 2. The XRD patterns of the pure and (Cu/Ag) doped TiO_2 nanoparticles.

Table1. XRD results of pure and (Cu/Ag) doped TiO_2 nanoparticles.

Sample	Wt. % Cu	Wt.% Ag	Cell parameter(A°)		Cell volume (A^3)	The main peak	Average crystallite size (nm)
			a=b	c			
T_0	0	0	3.779	9.158	130.79	25.477	13.56
T_1	1.5	1	3.782	9.346	133.67	25.386	12.73
T_2	1	1.5	3.775	9.389	133.76	25.413	13.03
T_3	1	1	3.788	9.609	137.87	25.253	12.67

Field emission scanning electron microscope (FESEM) and energy dispersive Xray-spectroscopy (EDX) analysis

The morphology analysis of the Cu/Ag-co-doped TiO_2 NPs was done by the FESEM technique. The FESEM micrographs of pure and Cu/Ag-doped TiO_2 NPs annealed at 500 °C were illustrated in Fig. 4. FESEM micrographs indicated that a non-uniform distribution of particles, consisting of either individual particles or clusters of particles. Typically, all Cu/Ag-doped TiO_2 NPs have smaller particle sizes compared to pure TiO_2. The image

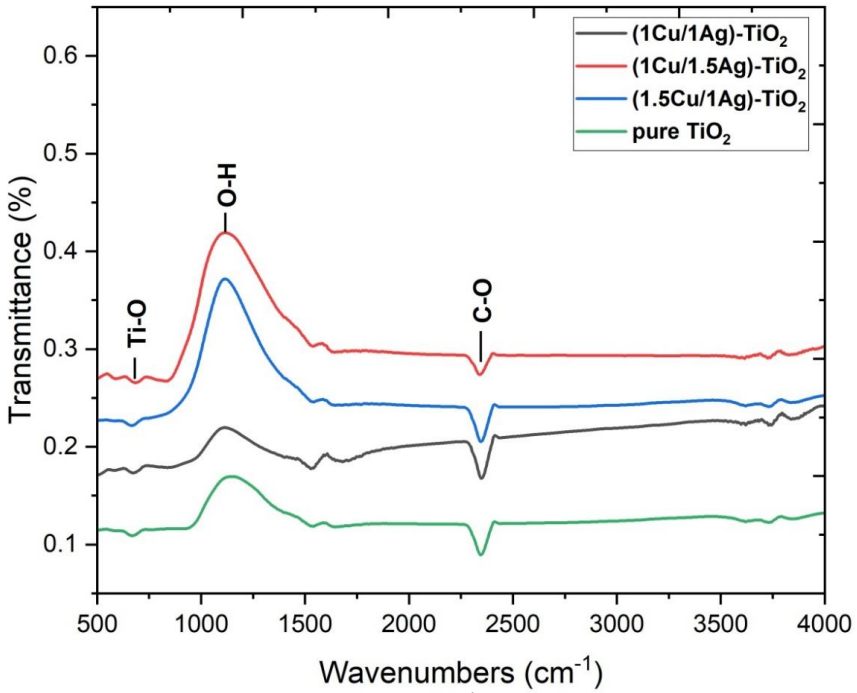

Fig. 3. FTIR spectra of the pure and (Cu/Ag) doped TiO_2 nanoparticles.

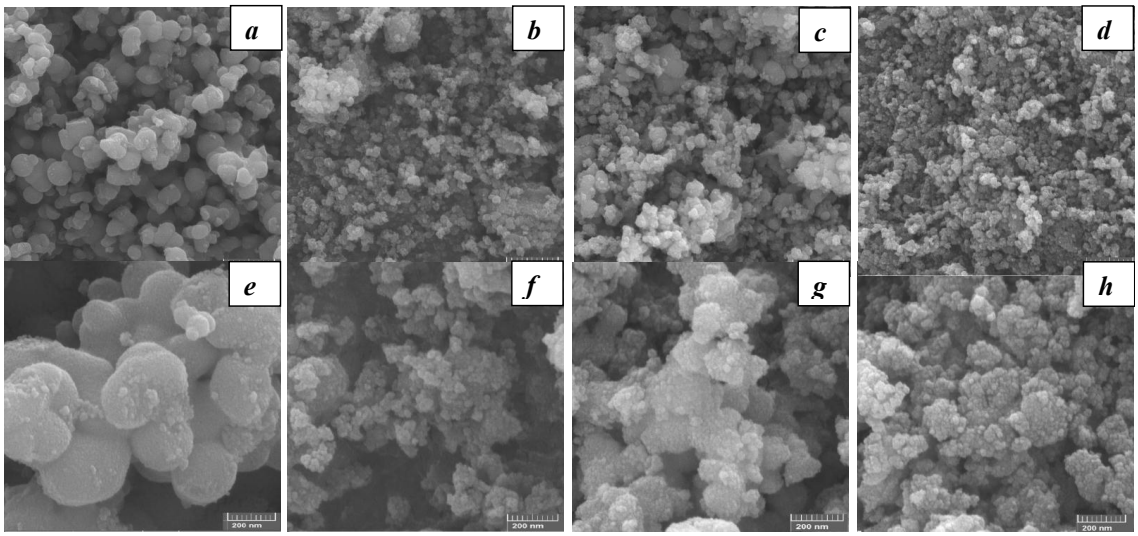

Fig. 4. FESEM micrographs of a) T_0, b) T_1, c) T_2, and d) T_3 samples low magnifications (X) while the lower panel represents their corresponding high magnification (X), respectively.

of FESEM displayed spherical particle shapes that were agglomerated in some extensions. These agglomerations were the result of reduced electrostatic repulsion due to the doping that changes the surface charge, which forced the particles to stick together. The average particle size was calculated from FESEM images utilizing Image J. The results revealed that the particle size decreased by doping. The average particle size of sample T_0 was observed to be 23.83 nm, but the particle sizes of samples T_1, T_2 and T_3 were 16.48 nm, 16.11 nm and 18.57 nm, respectively [35] [32].

EDX was used to investigate the microscopic composition of the Cu, Ag co-doped TiO_2 NPs. The EDX results of both un-doped and doped TiO_2 NPs are illustrated in Fig. 5. The EDX measurement qualitatively confirms the presence of titanium and oxygen in all synthesized nanoparticles. The doped NP Samples exhibited peaks of copper at 1 keV and silver at 3 keV. Consequently, it may be inferred that doping TiO_2 has been effectively

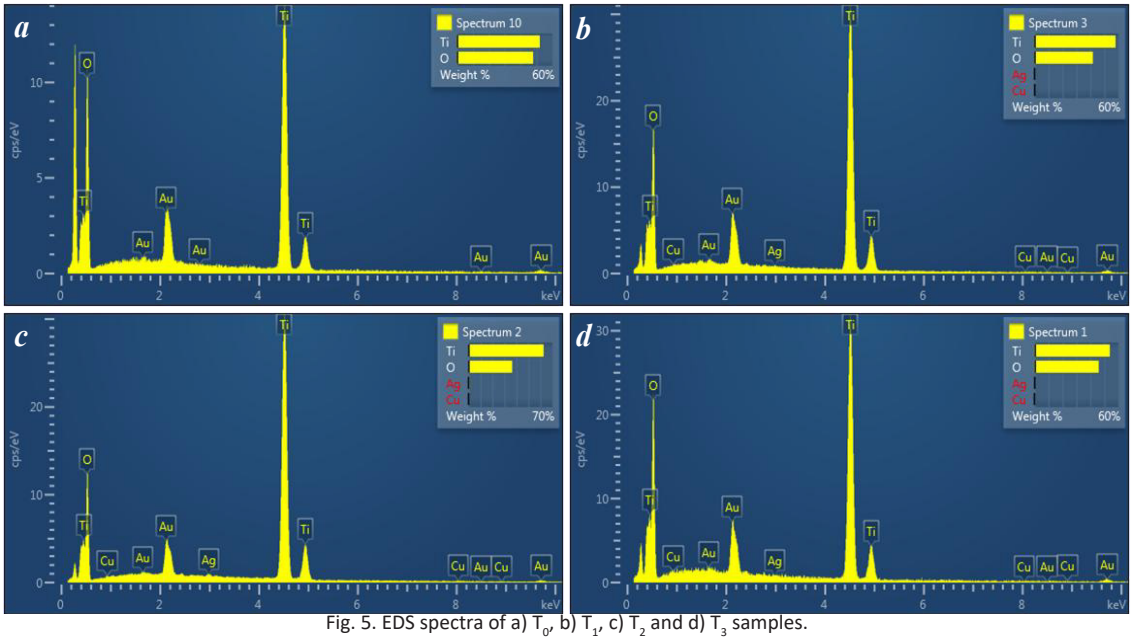

Fig. 5. EDS spectra of a) T_0, b) T_1, c) T_2 and d) T_3 samples.

Table 2. Atomic and weight percentages of elements in four different samples obtained via EDX spectroscopy.

Sample	Elements	Weight %	Atomic %
T_0	O	47.89	73.34
	Ti	52.11	26.66
	Cu	0	0
	Ag	0	0
T_1	O	41.67	68.20
	Ti	57.92	31.66
	Cu	0.20	0.08
	Ag	0.21	0.05
T_2	O	36.40	63.31
	Ti	62.62	36.38
	Cu	0.32	0.14
	Ag	0.66	0.17
T_3	O	45.87	71.79
	Ti	53.87	28.15
	Cu	0.00	0.00
	Ag	0.26	0.06

accomplished. Atomic and weight percentages of elements were shown in Table 2.

To verify the deposition of Cu and Ag co-doped TiO_2 NPs, elemental mapping was performed and is shown in Fig. 6. Fig. 6a illustrates the mapping analysis of TiO_2, confirming the existence of titanium and oxygen elements without any contaminants. Figs. 5b, c, and d provide the mapping that indicates the existence and uniform distribution of Cu, Ag, Ti, and O.

Obviously, the EDX and mapping images show the presences of Cu and Ag, which means that their concentration or crystallite size may be too small for XRD to pick up, or they may be found as nanoscale clusters that don't produce typical diffraction peaks.

Photoluminescence (PL) spectroscopy analysis

Photoluminescence (PL) spectroscopy is an effective method for investigating the electronic structure of nanomaterial, the transfer behavior of photo-excited electron-hole pairs in semiconductors, and the recombination rate. Fig. 7 illustrates the PL spectra of pure and Cu/Ag-doped TiO_2 nanoparticles, excited at a wavelength of 320 nm. The emission peaks of pure TiO_2 closely resemble those of Cu/Ag-doped TiO_2; however, the photoluminescence intensity of Cu/Ag-doped TiO_2 decreases compared to that of pure TiO_2. The UV emission peaks at 380 and 385 nm are regarded as the band edge emission of the host TiO_2, attributed to self-trapped excitations localized within TiO_6 octahedra. [36]. The emission

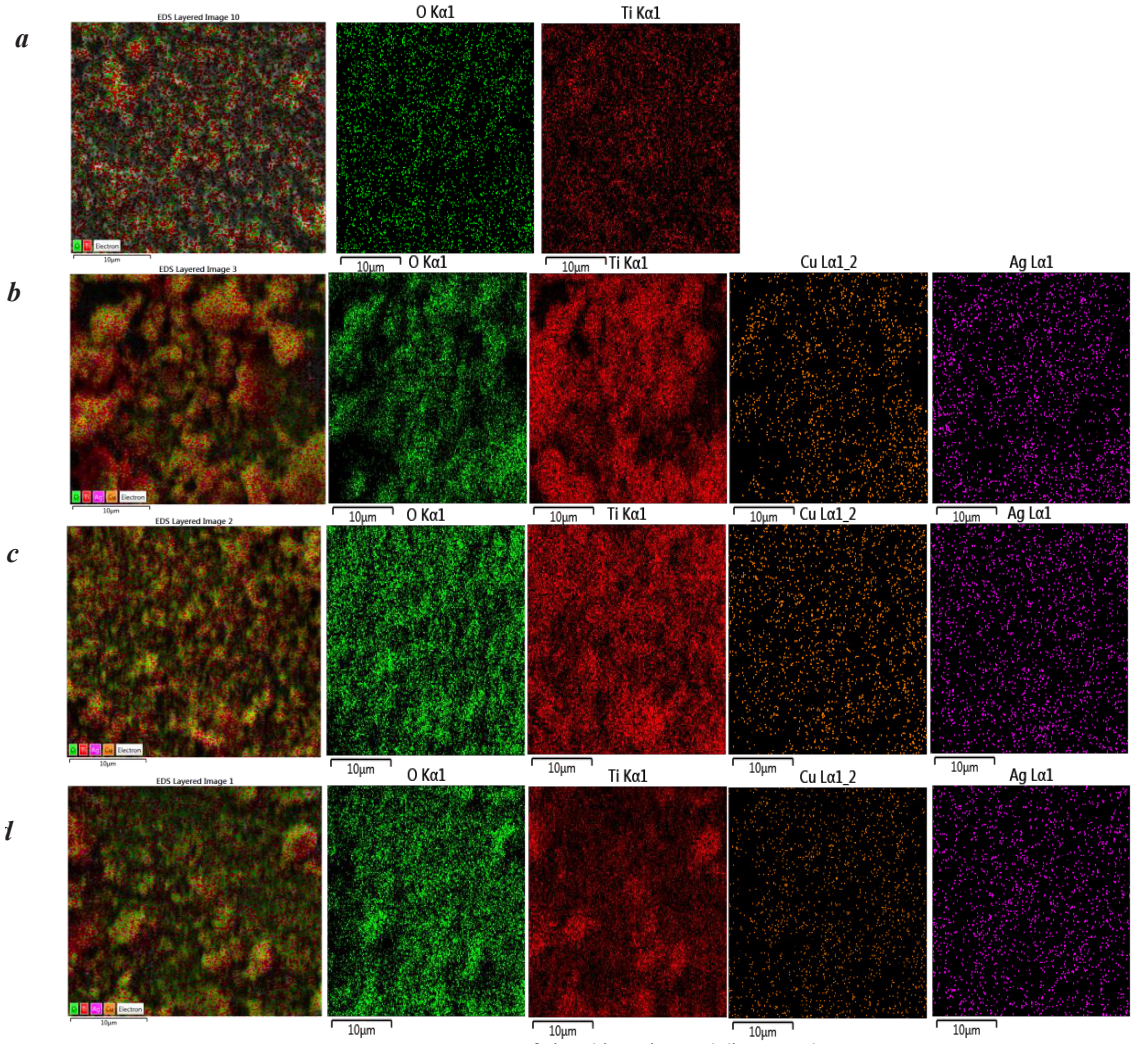

Fig. 6. mapping spectrum of a) T_0, b) T_1, c) T_2 and d) T_3 samples.

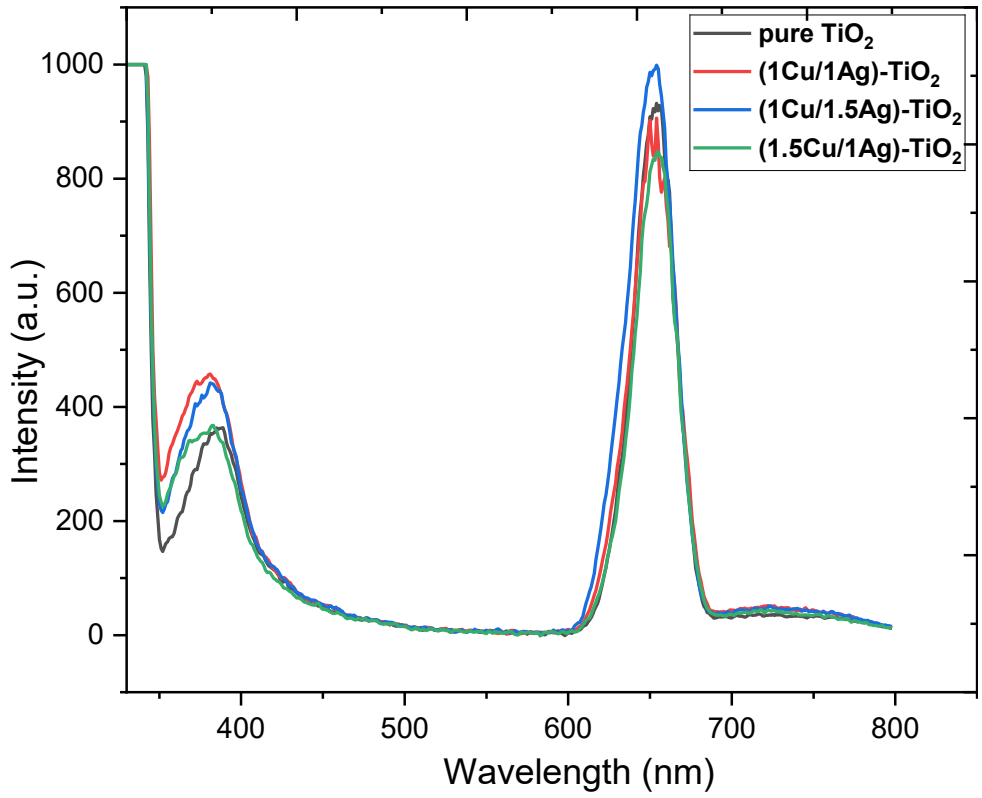

Fig. 7. Photoluminescence spectra of TiO_2 nanoparticles with different Cu/Ag concentrations.

peak in the range of 630–650 nm can be attributed to generated electron-hole pairs. These charge carriers may get trapped in defect states, such as oxygen vacancies, within the TiO_2 lattice. The recombination of these trapped carriers can result in visible light emission, including wavelengths around 630 nm [37]. Moreover, TiO_2 nanoparticles often exhibit surface states due to their high surface-to-volume ratio. These surface states can trap electrons or holes, and their recombination can lead to emissions in the visible spectrum [38]. In compounds containing copper, it is observed that with increasing weight percentage of copper, the emission intensity decreases and as a result, the recombination decreases [39]. At the same time, in compounds where Ag was doped to TiO_2, it was observed that the emission intensity, i.e. the rate of electron-hole rearrangement, increased with increasing weight percentage.

CONCLUSION

Titanium dioxide nanoparticles doped with different concentration of Cu and Ag, were synthesized using the solvothermal method, and annealed at 500 °C for 2 hours. The structural morphological and optical properties were investigated by XRD, FTIR, FESEM and PL. XRD analysis revealed that a shift of the main diffraction peak toward lower 2θ value and decreasing in crystallite size upon Ag and Cu doping compared to the un-doped sample, indicating lattice strain and structural distortion. The FESEM images showed that the distinctive spherical structure of the obtained nanoparticles with aggregation of tiny crystals. Future research on titanium dioxide doped with Cu and Ag holds significant promise for enhancing the materials properties and broadening its applications in photocatalysis, energy storage and environmental remediation.

CONFLICT OF INTEREST

The authors declare that there is no conflict of interests regarding the publication of this manuscript.

REFERENCE

1. Malik S, Muhammad K, Waheed Y. Nanotechnology: A Revolution in Modern Industry. Molecules. 2023;28(2):661.
2. Hamrayev H, Korpayev S, Shameli K. Advances in Synthesis

Techniques and Environmental Applications of TiO_2 Nanoparticles for Wastewater Treatment: A Review. Journal of Research in Nanoscience and Nanotechnology. 2024;12(1):1-24.
3. Sarkar MB, Mondal A, Choudhuri B, Mahajan BK, Chakrabartty S, Ngangbam C. Enlarged broad band photodetection using Indium doped TiO_2 alloy thin film. J Alloys Compd. 2014;615:440-445.
4. Zhao W, Wang W, Feng X, He L, Cao Q, Luan C, et al. Preparation and characterization of transparent indium- doped TiO 2 films deposited by MOCVD. Ceram Int. 2017;43(11):8391-8395.
5. Sugumaran S, Bellan CS. Transparent nano composite PVA–TiO_2 and PMMA–TiO_2 thin films: Optical and dielectric properties. Optik. 2014;125(18):5128-5133.
6. Horzum S, Gürakar S, Serin T. Investigation of the structural and optical properties of copper-titanium oxide thin films produced by changing the amount of copper. Thin Solid Films. 2019;685:293-298.
7. Badoni A, Sharma R, Prakash J. Titanium Dioxide Based Functional Materials for Antibacterial and Antiviral Applications. ACS Symposium Series: American Chemical Society; 2024. p. 257-280.
8. Yıldırım M. Characterization of the framework of Cu doped TiO_2 layers: An insight into optical, electrical and photodiode parameters. J Alloys Compd. 2019;773:890-904.
9. Liu J, Li Y, Arumugam S, Tudor J, Beeby S. Investigation of Low Temperature Processed Titanium Dioxide (TiO_2) Films for Printed Dye Sensitized Solar Cells (DSSCs) for Large Area Flexible Applications. Materials Today: Proceedings. 2018;5(5):13846-13854.
10. Kumar M, Gupta AK, Kumar D. Mg-doped TiO_2 thin films deposited by low cost technique for CO gas monitoring. Ceram Int. 2016;42(1):405-410.
11. Sakar M, Mithun Prakash R, Do T-O. Insights into the TiO_2-Based Photocatalytic Systems and Their Mechanisms. Catalysts. 2019;9(8):680.
12. Khan MM, Ansari SA, Pradhan D, Ansari MO, Han DH, Lee J, et al. Band gap engineered TiO_2 nanoparticles for visible light induced photoelectrochemical and photocatalytic studies. J Mater Chem A. 2014;2(3):637-644.
13. Barakat NAM, Kanjwal MA, Al-Deyab SS, Chronakis IS. Influences of Silver-Doping on the Crystal Structure, Morphology and Photocatalytic Activity of TiO_2 Nanofibers. Materials Sciences and Applications. 2011;02(09):1188-1193.
14. Nguyen Thi Thu T, Nguyen Thi N, Tran Quang V, Nguyen Hong K, Nguyen Minh T, Le Thi Hoai N. Synthesis, characterisation, and effect of pH on degradation of dyes of copper-doped TiO_2. J Exp Nanosci. 2015;11(3):226-238.
15. Mathew S, Ganguly P, Rhatigan S, Kumaravel V, Byrne C, Hinder SJ, et al. Cu-Doped TiO_2: Visible Light Assisted Photocatalytic Antimicrobial Activity. Applied Sciences. 2018;8(11):2067.
16. Wysocka I, Kowalska E, Ryl J, Nowaczyk G, Zielińska-Jurek A. Morphology, Photocatalytic and Antimicrobial Properties of TiO_2 Modified with Mono- and Bimetallic Copper, Platinum and Silver Nanoparticles. Nanomaterials. 2019;9(8):1129.
17. M KK, K B, G N, B S, A V. Plasmonic resonance nature of Ag-Cu/TiO_2 photocatalyst under solar and artificial light: Synthesis, characterization and evaluation of H_2O splitting activity. Applied Catalysis B: Environmental. 2016;199:282-291.
18. Majeed I, Ali H, Idrees A, Arif A, Ashraf W, Rasul S, et al. Understanding the role of metal supported on TiO_2 in photoreforming of oxygenates. Energy Advances. 2022;1(11):842-867.
19. Vargas Hernández J, Coste S, García Murillo A, Carrillo Romo F, Kassiba A. Effects of metal doping (Cu, Ag, Eu) on the electronic and optical behavior of nanostructured TiO_2. J Alloys Compd. 2017;710:355-363.
20. Qian H, Yuan B, Liu Y, Zhu R, Luan W, Zhang C. Oxygen vacancy enhanced photocatalytic activity of Cu_2O/TiO_2 heterojunction. iScience. 2024;27(5):109578.
21. Yuzer B, Aydın MI, Con AH, Inan H, Can S, Selcuk H, et al. Photocatalytic, self-cleaning and antibacterial properties of Cu(II) doped TiO_2. J Environ Manage. 2022;302:114023.
22. Mamunur Rashid M, Tomšič B, Simončič B, Jerman I, Štular D, Zorc M. Sustainable and cost-effective functionalization of textile surfaces with Ag-doped TiO_2/polysiloxane hybrid nanocomposite for UV protection, antibacterial and self-cleaning properties. Appl Surf Sci. 2022;595:153521.
23. Lee D-S, Chen Y-W. Nano Ag/TiO_2 catalyst prepared by chemical deposition and its photocatalytic activity. Journal of the Taiwan Institute of Chemical Engineers. 2014;45(2):705-712.
24. Alwan MH, Yaseen HM, Tahir KJ, Jabar BA. Emission Cross Sections of Eu3+ doped TiO_2 Prepared via Sol-Gel. Journal of Physics: Conference Series. 2019;1279(1):012002.
25. Zhang Y, Wang T, Zhou M, Wang Y, Zhang Z. Hydrothermal preparation of Ag-TiO_2 nanostructures with exposed {001}/{101} facets for enhancing visible light photocatalytic activity. Ceram Int. 2017;43(3):3118-3126.
26. Jalawkhan RS, Alosfur FKM, Abdul-Lettif AM. Characterization of pure anatase TiO_2 nano rods synthesized by microwave method. AIP Conference Proceedings: AIP Publishing; 2022. p. 030020.
27. Alosfur FKM, Ouda AA, Ridha NJ, Abud SH. Structure and optical properties of TiO_2 nanorods prepared using polyol solvothermal method. AIP Conference Proceedings: AIP Publishing; 2019. p. 030025.
28. SiO_2@TiO_2:Eu^{3+} and Its Derivatives: Design, Synthesis, and Properties. American Chemical Society (ACS).
29. Patel SKS, Jena P, Gajbhiye NS. Structural and room-temperature ferromagnetic properties of pure and Ni-doped TiO2 nanotubes. Materials Today: Proceedings. 2019;15:388-393.
30. Prajapat K, Mahajan U, Dhonde M, Sahu K, Shirage PM. Synthesis and characterization of TiO_2 nanoparticles: Unraveling the influence of copper doping on structural, surface morphology, and optical properties. Chemical Physics Impact. 2024;8:100607.
31. Zhang W, Liu Y, Yu B, Zhang J, Liang W. Effects of silver substrates on the visible light photocatalytic activities of copper-doped titanium dioxide thin films. Mater Sci Semicond Process. 2015;30:527-534.
32. Ali T, Ahmed A, Alam U, Uddin I, Tripathi P, Muneer M. Enhanced photocatalytic and antibacterial activities of Ag-doped TiO_2 nanoparticles under visible light. Materials Chemistry and Physics. 2018;212:325-335.
33. Huseynov EM, Huseynova EA. Infrared spectroscopy of nanocrystalline anatase (TiO_2) particles under the neutron irradiation. Opt Mater. 2023;144:114351.
34. Munir T, Sharif M, Ali H, Kashif M, Sohail A, Sabir N, Amin N, Mahmood A, Ahmed N. Impact of silver dopant on structural and optical properties of TiO_2 nanoparticles. Dig. J. Nanomater. Biostructures. 2019 ;14:279-284.
35. Alvaro RJ, Diana ND, Maria AM. Effect of Cu on optical properties of TiO_2 nanoparticles. Contemporary Engineering Sciences. 2017;10(31):1539-1549.
36. Senthil Kumar R, Gnanavel B. High performance catalytic activity of pure and silver (Ag) doped TiO_2 nanoparticles by a novel microwave irradiation technique. Journal of Materials Science: Materials in Electronics. 2016;28(5):4253-4259.
37. Shi J, Wang X, Feng Z, Chen T, Chen J, Li C. Photoluminescence Spectroscopic Studies on TiO_2 Photocatalyst. Nanostructure Science and Technology: Springer New York; 2010. p. 185-203.
38. Mathew S, kumar Prasad A, Benoy T, Rakesh PP, Hari M, Libish TM, et al. UV-Visible Photoluminescence of TiO_2 Nanoparticles Prepared by Hydrothermal Method. Journal of Fluorescence. 2012;22(6):1563-1569.
39. Dorraj M, Alizadeh M, Sairi NA, Basirun WJ, Goh BT, Woi PM, et al. Enhanced visible light photocatalytic activity of copper-doped titanium oxide–zinc oxide heterojunction for methyl orange degradation. Appl Surf Sci. 2017;414:251-261.